Study of distillation temperatures curves from Brazilian crude oil by 1H NMR-PLS

Lucas Mattos Duarte, Paulo Roberto Filgueiras, Julio Cesar Magalhaes Dias, Lize M. S. L. Oliveira, Eustaquio Vinicius Ribeiro Castro, and Marcone Augusto Leal de Oliveira

Just Accepted

Study of distillation temperatures curves from Brazilian crude oil by ^{1}H NMR-PLS

Lucas M. Duarte[a]*, Paulo R. Filgueiras[b], Júlio C. M. Dias[c], Lize M. S. L. Oliveira[c], Eustáquio V. R. Castro[b], Marcone A. L. de Oliveira[a]*

[a] Analytical chemistry and chemometrics group – GQAQ, Departament of Chemistry, Institute of Exact Sciences, Federal University of Juiz de Fora, University city, CEP 36036-330, Juiz de Fora, MG, Brazil
[b] Center of Competence in Petroleum Chemistry – NCQP, Laboratory of Research and Development of Methodologies for Analysis of Oils - LabPetro, Chemistry Department, Federal University of Espírito Santo, Av. Fernando Ferrari, 514, CEP: 29075-910, Vitória, Espírito Santo, Brazil.
[c] CENPES/PETROBRAS, CEP 21941-598, Rio de Janeiro, RJ, Brazil

*Corresponding authors: Lucas M. Duarte, e-mail: lucas.mtduarte@gmail.com and

Marcone A. L. de Oliveira, e-mail: marcone.oliveira@ufjf.edu.br and. Tel.: 32

21023309; fax: 32 21023310

1
2
3 **ABSTRACT**

2

3 An alternative method to predict distillation temperatures (DT) in Brazilian crude oil

4 samples using ^{1}H nuclear magnetic resonance spectroscopy (^{1}H NMR) in association

5 with partial least square (PLS) regression is proposed. From the acquisition of ^{1}H NMR

6 spectrum of seventy-four crude oil samples along with their distillation temperatures

7 (DT) obtained by Gas Chromatography, PLS models were built to predict DT from 5%

8 to 90% of distilled. In calibration and prediction steps, coefficients of multiple

9 determination (R^2) and root mean square errors (RMSE) were monitored throughout the

10 studied range. RMSEP% was the most important modeling parameter monitored,

11 showing a decreasing behavior across the studied range and present values lower than

12 5% for some models. The residual analysis through bias and nonparametric permutation

13 tests were taken into account for each built model. Lastly, the curves of DT estimated

14 by chemometrics, named DTEC, were faced to SimDis for each prediction sample. The

15 developed methodology by ^{1}H NMR-PLS can be successfully applied to Brazilian and

16 similar crude oil samples in order to determine DT from 5% to 90% of distilled.

17
18
19
20
21
22
23
24
25
26
27
28
29
30
31
32
33
34
35
36
37

1
2
3   **1   INTRODUCTION**
4
5
6   Distillation is the most important process in the petroleum industry.
7   Experimental information about boiling points distribution of crude oils and chemical
8   species coming from oil refining are considered essentials for monitoring, control and
9   product quality assurance. Simulated distillation (SimDis) by gas chromatography
10   emerged in the early sixties in order to evaluate the volatility curve of petroleum and its
11   distilled fractions[1]. Low sample amounts and quickness in achieving results corroborate
12   to the dissemination of this analytical technique as a safe alternative to the conventional
13   method available at the time, *i.e.*, the true boiling point (TBP) curve obtained by
14   standard distillation ASTM D2892 and D5236.

15   SimDis is a critical parameter in crude oil characterization. It is possible to know
16   fraction contents that crude is going to yield through this analysis. SimDis contributes
17   significantly to crude oil monetary evaluation combined with some important
18   physicochemical properties, such as API gravity. Although SimDis has been very well
19   established making the effective distillation cuts understood, the use of new, alternative
20   and advanced analytical methodologies promotes growing in the crude oil
21   characterization bringing improvements to the oil business.

22   In a general way, spectroscopic techniques have been highlighted as a powerful
23   analytical alternative to conventional methods to the determination of analytes and
24   properties in several complex samples presenting similar or better results to efficiency,
25   quickness and, several times, absence or minimization of sample pretreatment steps.
26   However, after the instrumental acquisition, the main challenge is properly handling the
27   huge amount of generated data. Thus, the chemometric approach is useful to overcome
28   these drawbacks. Taking into account crude oil physicochemical properties
29   determination, the most common scientific reports found in the literature consider near
30   infrared (NIR) and medium infrared (MIR) spectroscopy in association with partial least
31   squares (PLS) regression as a powerful alternative methodology[2–10]. Besides that,
32   nuclear magnetic resonance (NMR) spectroscopy also has gained prominence in
33   petroleum characterization[11–15].

34   In a recent work, we showed that it is possible to estimate API gravity, carbon
        residue, wax appearance temperature and basic organic nitrogen from a single ^{1}H NMR
        crude oil spectrum using a simple PLS[16]. Some other works approached different
        physicochemical properties from ^{1}H NMR associated with chemometrics[17–20]. Filgueiras

1   *et al.* performed work taking into account three distillation temperatures (DT)

2   equivalent to 10%, 50% and 90% distilled in Brazilian crude oil, whose main goal was

3   to establish confidence intervals for support vector regression (SVR) through boosting-

4   type ensemble method[21]. Considering diesel samples, Galvão *et al.* predicted DT

5   equivalent to 10% and 90% using NIR associated with different multivariate calibration

6   approaches[22] while Lira *et al.* DT equal to 50% and 85% using NIR and MIR[23].

7   Within this context, the aim of the present work was to predict eighteen DT from

8   5% to 90% w/w of distilled petroleum from different oil fields in Brazilian sedimentary

9   basin using ^{1}H NMR associated with PLS. The internal and global validation of the

10   built models considering the main multivariate statistical parameters and residuals

11   analysis of predicted values were assessed according to bias and permutation tests to

12   evaluate systematic and tendentious errors. SimDis and distillation temperature

13   estimated by chemometrics (DTEC) curves were faced and relative errors discussed.

14

2　EXPERIMENTAL SECTION

2.1　Samples and reference method

For the present study, seventy-four samples from different oil fields in Brazilian sedimentary basin covering a broad range of crudes type composed a dataset. Regarding API gravity, the dataset was composed from very light to very heavy crude oils and, besides that, other important physicochemical properties reveal this variety, as can be seen in **Table 1**. To use different types of crudes means to include variability in models, which makes them more robust and applicable.

DT for each 5% in mass of distilled for all 74 samples were obtained by high-temperature gas chromatography according to the standard analytical procedure described in ASTM D 7169. Altogether, eighteen DT were acquired by reference method and posteriorly estimated by proposed ^{1}H NMR-PLS method within the range from 5% to 90% w/w with the interval of 5% w/w between each level.

{INSERT TABLE 1}

Label: **Table 1 (In the end of this manuscript)**

Caption: **Some physicochemical properties of crude oil database**

2.2　^{1}H NMR measurements

^{1}H-NMR spectrum for individual crude oil sample was acquired on a Varian spectrometer VRMNS 400 model (Varian Inc., Palo Alto, CA – USA), operating with a magnetic field of 9.4 T using a 5 mm BroadBand probe 1H/19F/X, at 25 °C. A spectral window of 6,410.3 Hz, the acquisition time of 2.556 s, waiting time of 1 s, pulse of 90° (11,7 μs) and transient numbers equal to 64 were set. The experimental protocol follows these steps: 1) to weight 30 mg of sample; and 2) to solubilize in 550 μL of dichloromethane-d2 (CD_2Cl_2); and then 3) to transfer to probe and performed the instrumental measurement.

1   2.3   Chemometric approach

2

3   As described in sections 2.1 and 2.2, eighteen DT and ^{1}H NMR spectra were

4   acquired for each one of seventy-four samples. These results were grouped in eighteen

5   Y vectors and just one X matrix respectively, where X contains variables (instrumental

6   responses) and Y contains the property of interest to be modeled to build eighteen PLS1

7   models. One model was built to estimate each temperature. PLS is a multivariate

8   quantitative method for relating two data matrices, X and Y, using a linear model that

9   goes beyond traditional regressions, which also models X and Y structures [24]. All

10   models were built following the same procedure.

11   Initially, raw spectral set (**Figure 1**) corresponding to sample dataset and three

12   spectra of light, medium and heavy crude oil, representing their great variety, were

13   visually evaluated in order to understand the instrumental response to samples.

14   Knowing that alignment is an important step when NMR is used to multivariate

15   purposes[25], icoshift tool[26] was employed, and the result is shown in **Figure 2**. Besides

16   alignment, the standard normal variate (SNV)[27] procedure was used as preprocessing in

17   order to have a better baseline adjust. The preprocessing step contributes significantly to

18   the process, finding more robust, accurate and parsimonious models, since the spectral

19   perturbations (undesirable variations) caused mainly by matrix interferents are

20   substantially attenuated[28].

21

22   **{INSERT FIGURES 1 AND 2}**

23

24

25   Label**: Figure 1 (View file attached)**

26   Caption: **Aligned ^{1}H NMR spectra for three types of crude oils (A) and for all 74**
27   **samples composing the dataset (B)**

28

29

30   Label**: Figure 2 (View file attached)**

31   Caption: **^{1}H NMR region approximated raw (A) and aligned full crude oil dataset**

32   **spectra (B)**

33

34

1   Dataset was split into calibration (70% of original samples) and prediction (other

2   30%) using Kennard-Stone (KS) algorithm[29]. Calibration subset was trained, and

3   evaluated through an internal procedure by 5-fold cross-validation method and the

4   number of optimal latent variables (LVs) was defined according to the root mean square

5   error of cross validation (RMSECV). It is important to highlight that not always optimal

6   LVs were selected with lowest RMSECV value, being the predictive step taken into

7   consideration.

8   An important consideration when a multivariate method is developed for

9   calibration purposes is the global validation step. Thus, 30% independent samples

10   dedicated to prediction were used and root mean square error of prediction (RMSEP)

11   was the most important parameter monitored. Both RMSECV and RMSEP were

12   described by the same mathematical equation, within each respective step, can be

13   written as

14

15    $$RMSE = \sqrt{\frac{\sum_{i=1}^{n}(y_{p,i}-y_{r,i})^2}{n}} \quad (1)$$

16

17   where $y_{p,i}$ and $y_{r,i}$ are predicted and reference values for i^{th} sample and n is the number

18   of samples of the calibration or prediction subset evaluated. The global model's

19   accuracy is given by RMSEP, however, in this case, it is not simple analyze its values

20   purely due to magnitude increase with distilled percentage. An elegant boundary

21   condition to discuss and compare global model errors across distillation curve is

22   working with

23

24    $$RMSEP\% = \frac{RMSEP}{\bar{y}_p} 100 \quad (2)$$

25   where RMSEP is normalized by the average of all prediction values ($\bar{y}_p$). Besides that,

26   the correlation between predicted and reference values for both steps is also an

27   important statistics parameter. Therefore, the coefficient of multiple determination for

28   calibration (R^2_c), cross-validation (R^2_{cv}) and prediction (R^2_p) was evaluated as

29

30    $$R^2 = 1 - \frac{\sum_i(y_{r,i}-y_{p,i})^2}{\sum_i(y_{r,i}-\bar{y}_r)^2} \quad (3)$$

31

1   where $y_{p,i}$ and $y_{r,i}$ refers to the predicted and reference values for ith sample

2   respectively, while $\bar{y}_r$ is the mean vector containing reference values.

3   For all models, from 5% to 90% of distilled, residual analysis by bias test[30] and

4   nonparametric permutation test [31] were made. In the first test, it is possible to access the

5   systematic errors that affect the estimate always in the same direction, leading to results

6   above or below the expected. The second evaluate trends, and for this case, linear and

7   quadratic functions were used in order to describe reordered reference values against the

8   original residues related to each predicted value (maintained order).

9   After the aforementioned statistical parameters have been evaluated, as the main

10   result, SimDis and DTEC curves were faced and relative error (RE), in each DT

11   predicted by the model, were showed in the second y-axis:

12

13   $$RE(\%) = \frac{|y_p - y_r|}{y_r} 100 \quad (4)$$

14

3 RESULTS AND DISCUSSIONS

3.1 Individual models

Building models for all DT followed the same strategy as pointed out in section 2.3. The most important parameters for both steps, calibration and prediction, are presented in four graphics in **Figure 3**. Taking into account calibration step, with the increase of distilled percentage, RMSECV increasing to 75% due to the natural growth in DT according to depicted in graphic D. However, in the three last points corresponding to models for 80, 85 and 90% of distilled, a great leap is observed. This growth is similar to the behavior for LVs and by a decrease for the same three points of R^2_{cv}, as shown in the graphics B and A, respectively. Another parameter in calibration step to be noted is the R^2_c (graphic A) since its curve ascends slightly with the natural increase in DT. This result is interesting because the R^2_c is better fitted than R^2_{cv}. The R^2_{cv} is more reliable due to the 5-fold cross-validation while the R^2_c apply the calibration equation directly on the calibration subset, providing over-optimistic results. Actually, in the last distilled percentages, the variability decreases because the DT approaching, reflecting in the R^2_{cv} and RMSECV analysis, which is supported by the increase in LVs across the distillation curve (graphic B).

The prediction step with separated test samples to validate the analytical procedure and achieves reliability to the proposed method were carried out. Analyzing the graphic A, was observed that R^2_p has a smooth decrease with an increase of distilled percentage. On the other hand, RMSEP curve (graphic D) presented a slightly increasing behavior due to the natural growth in DT. Nevertheless, RMSEP% provides a more interesting result since its values were normalized by the average vector y of each prediction subset from the respective model, because they were independent of the DT magnitude. Graphic C shows the RMSEP% decreasing behavior across the distillation models from 5% to 45%, where four LVs were used (graphic B), and this RMSEP% trend remains until the end of the distillation, with the increase in LVs from 50%. It is important to clarify that the apparent disagreement between monitoring of RMSEP% and R^2_p does not match with the real situation. Graphic C presents the RMSEP% curve indicating that the global accuracy improves with distilled percentage, while graphic A points to adjust deterioration with R^2_p decrease, explained by KS separation. The KS algorithm is based on Euclidean norm, and the prediction subset presented samples with

1   certain closeness leading to a shorter range, negatively influencing over R^2_p values.

2   However, other partitioning methods were tested and was observed that KS method

3   resulted in lowers RMSEP taking a more accurate analytical method.

4

5   **{INSERT FIGURE 3}**

6

7   Label**: Figure 3 (View file attached)**

8   Caption: **Monitoring of multivariate statistic parameters across distilled percentage**

9   **(% w/w), being these: (A) R^2 for calibration, cross-validation and prediction, (B)**

10   **LVs, (C) RMSEP% and (D) RMSE for cross-validation and prediction**

11

12

13   3.2   Residual analysis

14

15   Two more monitoring across modeling to evaluate the residues were performed.

16   Bias test for residues of models from 5% to 90% distilled showed no systematic errors

17   since t calculated (t_{calc}) was lower than t critical (t_{crit}), and was equals to 2.08, according

18   to shown in the **Figure 4**, graphic A. In the bias test 95% confidence interval was

19   considered.

20   Applying nonparametric permutation test was observed that in all fitted models,

21   there are no linear and quadratic trends in their residues, since all p-values were greater

22   than significance error ($\alpha = 0.05$). This result shows that permuting 10,000 times y_r the

23   residues were randomly distributed around zero, as seen in **Figure 4**, graphic B.

24

25   **{INSERT FIGURE 4}**

26

27   Label**: Figure 4 (View file attached)**

28   Caption: **Monitoring of t_{calc} for bias test (A) and high order coefficient for**

29   **quadratic (b_2) and linear (b_1) functions for nonparametric permutation test (B)**

30   **across distilled percentage (% w/w)**

31

32

33

1

2

3   3.3   Comparison between SIMDIS and DTEC

4

5   The multivariate statistics analysis of validated models, described in sections 3.1 and 3.2, provided great reliability for results. Thus, DT estimated by validated PLS models were plotted against distilled percentage generating a curve with a very similar profile of SimDis, which was denominated DTEC. Therefore, DTEC and SimDis curves were overlapped and RE was calculated for all points.

       For all modeling, the dataset partitioning by KS algorithm begot twenty-two prediction samples, and all of them were compared to their referred SimDis as shown in **Figure 5** for an example of a crude oil sample with 29.4 API gravity. This graphic depicted an excellent agreement between DTEC and SimDis since the results obtained for RE is lower than 4%, and the great majority is around 1%. Another twenty-one predicted samples had DTEC and SimDis overlapped as shown in **Figure 6**. The prediction subset has samples with 17, 23.7, 28 and 34 API gravity, for example, demonstrating that different samples were considered. The sample with 28.7 API gravity presented the greater RE, around 27%; however, it happened just for the model referred to 5% of distilled, after that decrease to approximately 10%. This behavior was observed for other samples, where the initial point has a greater RE than other distilled percentages.

{INSERT FIGURES 5 AND 6}

Label**: Figure 5 (View file attached)**

Caption: **DTEC *vs* SimDis with RE for all DT points for a crude oil with 29.4 API gravity**

Label**: Figure 6 (View file attached)**

Caption: **DTEC *vs* SimDis with RE for all DT points for twenty-one crude oils with different API gravities. For all graphics left y-axis shows Distillations temperatures (°C), x-axis shows distilled (% w/w) and right y-axis relative error (%)**

11

1
2
3   **4   CONCLUSIONS**

4

5   The proposed ^{1}H NMR-PLS methodology was successfully applied to Brazilian

6   crude oil samples, from different provenances, which after a carefully multivariate

7   statistics parameters evaluation, allowed to predict eighteen distillation temperatures

8   referring to their respective distilled percentage. Coefficients of multiple determination,

9   and root mean square errors for both steps (calibration and prediction) were monitored

10   for all built models across the studied range, from 5% to 90% in mass of distilled.

11   RMSEP% was the most important modeling parameter monitored, reaching values

12   lower than 5% for models with distilled percentages greater than 55% and values lower

13   than 8% for lower than 55% of distilled, except the initial point (5% of distilled) with

14   RMSEP% equals to 12%. RMSEP% curve showed a decreasing behavior from 5% to

15   90% of distilled. Therefore, with estimated distillation temperatures for all percentage

16   distilled, DTEC curves were faced to respectives SimDis showing good agreement for

17   all twenty-two predicted samples with small relative errors for the vast majority of

18   distillation temperatures.

19   Therefore, taking a crude oil sample with similar characteristics that was used in

20   this work and obtaining a simple spectrum, it is possible to plot their distillation

21   temperature curve. This methodology presents as advantages the use of a small amount

22   of sample, quickness due to a short instrumental time analysis and robustness since

23   different samples were considered in the dataset.

12

1 **Aknowledgments**

2

3

1   **Table 1**: Some physicochemical properties of crude oil database

2

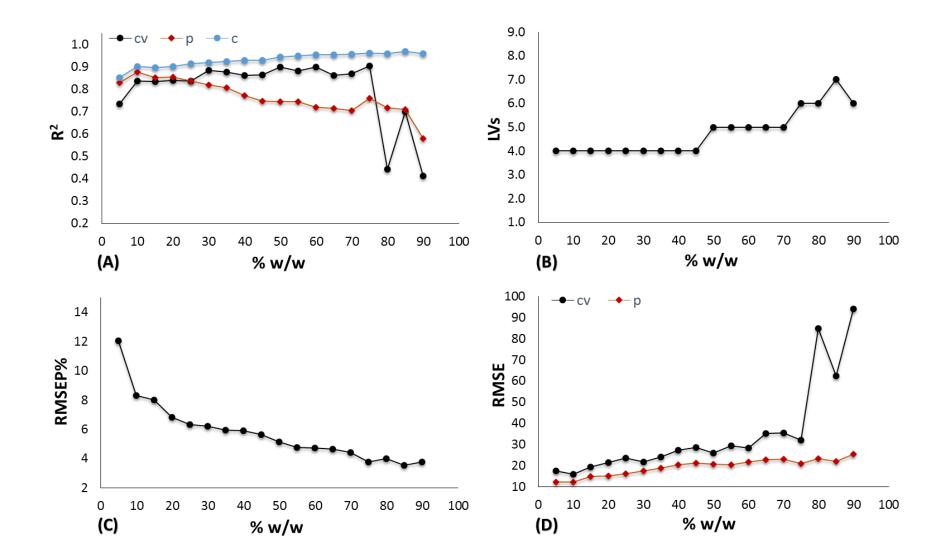| Physicochemical property	Range	Reference method
API gravity	13.1-54.0	ISO 12185
Viscosity at 30 °C (mm^2 s^{-1})	0.8-1118.0	ASTM D 7042
Saturates (% w/w)	36.6-90.6	SFC/TLC-FID
Aromatics (% w/w)	7.0-37.2	SFC/TLC-FID
Resins (% w/w)	4.8-42.8	SFC/TLC-FID
Asphaltenes (% w/w)	0.33-9.6	ASTM D 6560

3

14

1 **References**
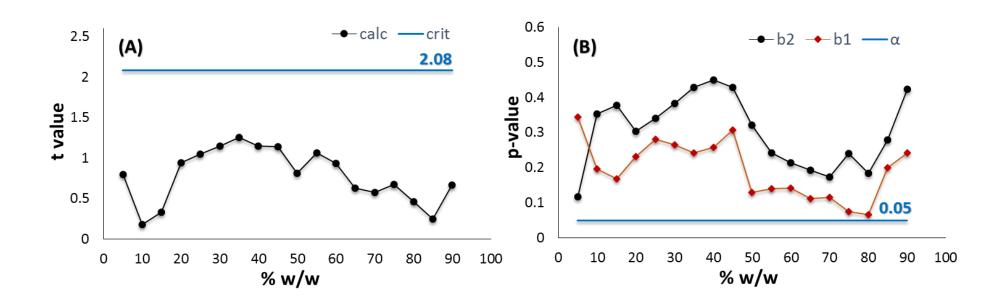
2

3 (1) Ferreira, A. de A.; Neto, F. R. de A. *Quim. Nova* **2005**, *28* (3), 478–482.

4 (2) Ruiz, M. D.; Bustamante, I. T.; Dago, A.; Hernández, N.; Núñez, A. C.; Porro, D.

5 *J. Chemom.* **2010**, *24* (7-8), 444–447.

6 (3) Khanmohammadi, M.; Garmarudi, A. B.; Garmarudi, A. B.; De la Guardia, M.

7 *TrAC - Trends Anal. Chem.* **2012**, *35*, 135–149.

8 (4) Müller, A. L. H.; Picoloto, R. S.; Mello, P. D. A.; Ferrão, M. F.; Dos Santos, M.

9 D. F. P.; Guimarães, R. C. L.; Müller, E. I.; Flores, E. M. M. *Spectrochim. Acta -*

10 *Part A Mol. Biomol. Spectrosc.* **2012**, *89*, 82–87.

11 (5) Filgueiras, P. R.; Sad, C. M. S.; Loureiro, A. R.; Santos, M. F. P.; Castro, E. V.

12 R.; Dias, J. C. M.; Poppi, R. J. *FUEL* **2014**, *116*, 123–130.

13 (6) Jingyan, L.; Xiaoli, C.; Songbai, T.; Wanzhen, L. *China Pet. Process.*

14 *Petrochemical Technol.* **2011**, *13* (4), 1–7.

15 (7) Jingyan, L.; Xiaoli, C.; Songbai, T. *Energy and Fuels* **2012**, *26* (9), 5633–5637.

16 (8) Laxalde, J.; Ruckebusch, C.; Devos, O.; Caillol, N.; Wahl, F.; Duponchel, L.

17 *Anal. Chim. Acta* **2011**, *705* (1-2), 227–234.

18 (9) Balabin, R. M.; Smirnov, S. V. *Anal. Chim. Acta* **2011**, *692* (1-2), 63–72.

19 (10) Abbas, O.; Rebufa, C.; Dupuy, N.; Permanyer, A.; Kister, J. *Fuel* **2012**, *98*, 5–14.

20 (11) Alam, T. M.; Alam, M. K. *Annu. Reports NMR Spectrosc.* **2004**, *54*, 41–80.

21 (12) Winning, H.; Larsen, F. H.; Bro, R.; Engelsen, S. B. *J. Magn. Reson.* **2008**, *190*

22 (1), 26–32.

23 (13) Silva, S. L.; Silva, A. M. S.; Ribeiro, J. C.; Martins, F. G.; Da Silva, F. A.; Silva,

24 C. M. *Anal. Chim. Acta* **2011**, *707* (1-2), 18–37.

25 (14) Filgueiras, P. R.; Portela, N. de A.; Silva, S. R. C.; Castro, E. V. R.; Oliveira, L.

26 M. S. L.; Dias, J. C. M.; Cunha Neto, A.; Romão, W.; Poppi, R. J. *Energy &*

27 *Fuels* **2016**, acs.energyfuels.5b02377.

28 (15) Barbosa, L. L.; Sad, C. M. S.; Morgan, V. G.; Figueiras, P. R.; Castro, E. R. V.

29 *Fuel* **2016**, *176*, 146–152.

30 (16) Duarte, L. M.; Filgueiras, P. R.; Silva, S. R. C.; Dias, J. C. M.; Oliveira, L. M. S.

31 L.; Castro, E. V. R.; de Oliveira, M. A. L. *Fuel* **2016**, *181*, 660–669.

32 (17) V, D. M.; Uribe, U. N.; Murgich, J. **2007**, No. 9, 1674–1680.

33 (18) Molina V, D.; Uribe, U. N.; Murgich, J. *Fuel* **2010**, *89* (1), 185–192.

34 (19) Masili, A.; Puligheddu, S.; Sassu, L.; Scano, P.; Lai, A. *Magn. Reson. Chem.*
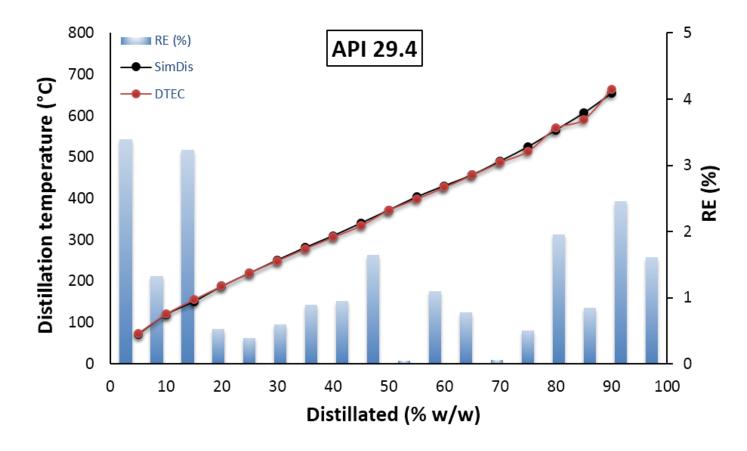
15

1   **2012**, *50* (11), 729–738.

2   (20)   de Peinder, P.; Visser, T.; Petrauskas, D. D.; Salvatori, F.; Soulimani, F.;

3   Weckhuysen, B. M. *Vib. Spectrosc.* **2009**, *51* (2), 205–212.

4   (21)   Filgueiras, P. R.; Terra, L. A.; Castro, E. V. R.; Oliveira, L. M. S. L.; Dias, J. C.

5   M.; Poppi, R. J. *Talanta* **2015**, *142*, 197–205.

6   (22)   Galvão, R. K. H.; Araújo, M. C. U.; Martins, M. D. N.; José, G. E.; Pontes, M. J.

7   C.; Silva, E. C.; Saldanha, T. C. B. *Chemom. Intell. Lab. Syst.* **2006**, *81* (1), 60–

8   67.

9   (23)   de Fátima Bezerra de Lira, L.; de Vasconcelos, F. V. C.; Pereira, C. F.; Paim, A.

10   P. S.; Stragevitch, L.; Pimentel, M. F. *Fuel* **2010**, *89* (2), 405–409.

11   (24)   Wold, S.; Sjostrom, M.; Eriksson, L. *Chemom. Intell. Lab. Syst.* **2001**, *58*, 109–

12   130.

13   (25)   Sousa, S. A. A.; Magalhães, A.; Ferreira, M. M. C. *Chemom. Intell. Lab. Syst.*

14   **2013**, *122*, 93–102.

15   (26)   Savorani, F.; Tomasi, G.; Engelsen, S. B. *J. Magn. Reson.* **2010**, *202* (2), 190–

16   202.

17   (27)   Barnes, R. J.; Dhanoa, M. S.; Lister, S. J. *Appl. Spectrosc.* **1989**, *43*, 772–777.

18   (28)   Sharma, S.; Goodarzi, M.; Ramon, H.; Saeys, W. *Talanta* **2014**, *121*, 105–112.

19   (29)   Kennard, R. W.; Stone, L. A. *Technometrics* **1969**, *11* (1), 137–148.

20   (30)   ASTM, E.-05. **2012**, 1–29.

21   (31)   Filgueiras, P. R.; Alves, J. C. L.; Sad, C. M. S.; Castro, E. V. R.; Dias, J. C. M.;

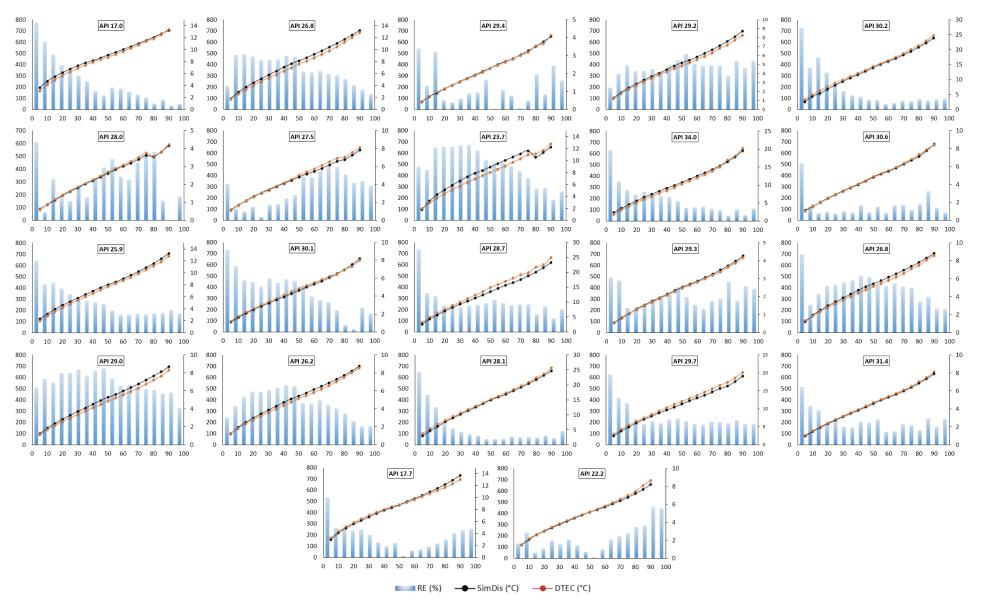22   Poppi, R. J. *Chemom. Intell. Lab. Syst.* **2014**, *133*, 33–41.

23

24

25

26

27

28

1
2
3
4
5
6
7
8
9
10
11
12
13
14
15
16
17
18
19
20
21
22
23
24
25
26
27
28
29
30
31
32
33
34
35
36
37
38
39
40
41
42
43
44
45
46
47

(A)

(B)

(C)

(D)